

Published in final edited form as:

Laryngoscope. 2013 November ; 123(11): . doi:10.1002/lary.24102.

Fluorescently labeled therapeutic antibodies for detection of microscopic melanoma

Kristine E. Day, MD¹, Lauren N. Beck, BS¹, Nicholas L. Deep, BS¹, Joy Kovar, MS², Kurt R Zinn, PhD DVM³, and Eben L. Rosenthal, MD¹

¹Department of Surgery, University of Alabama at Birmingham, Birmingham, AL 35294

²LI-COR Biosciences, Lincoln, NE, 68504

³Department of Radiology, University of Alabama at Birmingham, Birmingham, AL 35294

Abstract

Objective—Detection of microscopic disease during surgical resection of melanoma remains a significant challenge. To assess real-time optical imaging for visualization of microscopic cancer, we evaluated three FDA-approved therapeutic monoclonal antibodies.

Study Design—Prospective, basic science

Methods—Melanoma cell lines (A375 and SKMEL5) were xenografted into the ears of immunodeficient mice. Bevacizumab, panitumumab, tocilizumab, or a non-specific IgG were covalently linked to a near-infrared (NIR) fluorescent probe (IRDye800CW) and systemically injected. Primary tumors were imaged and then resected under fluorescent guidance using the SPY, an NIR imaging system used in plastic and reconstructive surgeries to evaluate perfusion. Mice were also imaged with the Pearl Impulse small animal imager, an NIR imaging system designed for use with IRDye800CW. Post-resection, small tissue fragments were fluorescently imaged and presence of tumor subsequently confirmed by correlation with histology.

Results—All fluorescently-labeled therapeutic monoclonal antibodies could adequately delineate tumor from normal tissue based on tumor-to-background ratios (TBR) compared to IgG-IRDye800CW. On serial imaging, panitumumab achieved the highest TBRs with both SPY and Pearl (3.8 and 6.6). When used to guide resections, the antibody-dye conjugates generated TBRs in the range of 1.3-2.2 (average=1.6) using the SPY and 1.9-6.3 (average=2.7) using the Pearl. There was no significant difference amongst the antibodies with either imaging modality or cell line (one-way ANOVA).

Conclusion—Our data suggests that FDA approved antibodies may be suitable targeting agents for the intraoperative fluorescent detection of melanoma.

Level of Evidence—N/A

Keywords

cutaneous; head and neck; optical imaging; surgery; melanoma; antibody; animal model; fluorescence

Corresponding Author: Eben L. Rosenthal, MD, Division of Otolaryngology, BDB Suite 563 1808 7th Avenue South, Birmingham, AL 35294-0012, Tel: (205) 934-9767, Fax: (205) 934-3993, oto@uab.edu.

Financial Disclosure: Work was supported by grants from NIDCR (R21DE019232) and NIH (T32CA091078-11). Equipment was donated by Novadaq and IRDye800CW was supplied by LI-COR Biosciences

Conflict of Interest: none

This work was presented at the Triological Society Combined Sections Meeting held in Scottsdale, AZ, January 25, 2013.

Introduction

While melanoma makes up only 3% of all skin cancers, it accounts for 83% of skin cancer deaths making it the most lethal form of skin cancer.¹ Head and neck melanoma in particular, has been shown to be more aggressive and carries an increased mortality rate compared to other locations.^{2,3} Currently, standard of care includes wide local excision with a gross margin of uninvolved surrounding tissue. Significant controversy, however, exists over the recommended width of margins needed for clearance.⁴ Immunostaining has been employed for more accurate detection of melanocytic disease, but this requires a significant amount of time and is associated with relatively high costs.^{5,6} Therefore, there is great interest in developing a technique to optimize positive margin detection intraoperatively. A real-time cancer imaging modality has the potential to improve patient outcomes through decreased positive margin rates, sparing of uninvolved tissue, and improved survival overall.

Imaging techniques using the near-infrared (700-900nm) region have emerged as a promising solution to intraoperative cancer detection and resection. Fluorophores, such as IRDye800CW, emitting light in the 800nm region have shown better tumor-to-background ratios (TBR) because of increased depth penetration and lower nonspecific fluorescence.⁷ The increased depth penetration of these fluorophores is of particular clinical relevance for melanoma where Breslow's thickness has prognostic implications. Concurrently, novel biomarkers and therapeutic targets for melanoma are emerging. Among them are epidermal growth factor receptor (EGFR) and vascular endothelial growth factor (VEGF), whose deregulated pathways have been implicated in the sustained proliferation, survival, invasion, and metastases of melanoma cells.⁸ Interleukin-6 receptor (IL-6R) has been suggested to be highly involved in melanoma development.⁹ Antibodies against these proteins (panitumumab, bevacizumab, and tocilizumab respectively) have already been developed and FDA approved. The use of monoclonal antibodies coupled to various fluorophores for imaging purposes have been reported in different tumor types.¹⁰⁻¹² It is unknown if fluorophore-labeled antibodies can be successfully used to improve margin status in malignant melanoma.

We hypothesize that both macroscopic and microscopic melanoma can be detected by a real-time intraoperative imaging system (SPY System, Novadaq, Toronto, Canada) using monoclonal antibodies conjugated to IRDye800CW. In addition, we seek to determine which fluorescently-labeled FDA-approved antibody (bevacizumab, panitumumab, or tocilizumab) has the optimal imaging properties in a preclinical murine model.

Materials and Methods

Cell Lines and Tissue Culture

A375 and SKMEL5 (ATCC, Manassas, VA) were the melanoma cell lines used. Tumor heterogeneity has become a challenge to development of targeted therapeutics or imaging agents and for tumor characterization. Therefore, we experimented with two different melanoma cell lines in order to validate the methodology and technology. Cells were grown and maintained in Dulbecco's modified Eagle's medium (DMEM) containing 10% fetal bovine serum (FBS), 1% penicillin, streptomycin, and amphotericin B. Cells were incubated at 37°C in 5% CO₂. 2×10⁶ cells in 200µL of phosphate buffer solution (PBS) were administered subcutaneously.

Reagents

Antibodies included bevacizumab (Avastin; Genentech, San Francisco, California; 149 kDa), panitumumab (Vectibix; Amgen, Thousand Oaks, California; 147 kDa), and

tocilizumab (Actemra; Genentech, San Francisco, California; 148 kDa) (Table 1). Control antibody was protein A purified IgG antibody (Innovative. Ir-Hu-Gf, #30010BM; 146kDa). Immunohistochemical analysis with HMB-45 (mouse monoclonal, catalog # ab787; Abcam, Cambridge, MA) was performed to confirm melanoma tumor cells. HMB-45 was chosen for its high specificity, though other immunohistochemical stains for melanoma are available. Staining was performed as previously described.¹³ IRDye800CW (IRDye800CW-*N*-hydroxysuccinimide ester; LI-COR Biosciences, Lincoln, Nebraska), with an absorption and emission peak of 778nm/794nm, was the fluorescent probe. Maximums decrease slightly (774nm/789nm) when conjugated to an antibody.¹⁴ Bevacizumab, panitumumab, tocilizumab, and IgG were labeled according to the manufacturers' protocol. This involved incubation with the IRDye800CW for 2h and removal of unconjugated dye by desalting columns (Pierce, Zeba, #89891).

Binding Affinity Assay

Binding affinity assays for each antibody were performed to determine if antigen specificities were retained after fluorescent labeling with IRDye800CW. 6 lanes of a 96-well black plate were coated with recombinant EGFR (rEGFR/ErbB1; 400ng/well/100 μ L; Fc Chimera, 344-ER), IL-6R (rIL-6R ; 400ng/well/100 μ L; 227-SR/CF), or VEGF (rVEGF; 100ng/well/100 μ L; 293-VE/CF) overnight at 4°C. Wells were blocked for 1h at RT with 1% bovine serum albumin (BSA), then washed with PBS 3x. For control, purified antibody was added to 3 lanes of coated wells and allowed to block for 1h. Serial dilutions of labeled antibody (0.234375-30 nM for bevacizumab and tocilizumab; 0.05-6.7 nM for panitumumab) were then added to all coated wells and incubated for 1h. Uncoated wells on the same plate were also maintained for background control. After incubation, wells were washed with PBS and imaged using the Pearl Impulse imager (LI-COR Biosciences, Lincoln, Nebraska). Well intensities were quantified using the Pearl Impulse software, version 2.0.

Animal Models

Nude (nu/nu) and severe combined immunodeficient (SCID) female mice (Charles River Laboratories, Hartford, CT), aged 4-6 weeks, were housed in accordance with the Institutional Animal Care and Use Committee (IACUC) guidelines. All experiments were conducted and mice euthanized according to IACUC guidelines.

Table 2 outlines our mice experiments. 4 flank model mice received injections of A375 cells and tumor size was monitored weekly until they reached 25mm². The flank model was chosen for the initial site in the first 4 mice in order to evaluate if the antibody-dye conjugates would localize and fluoresce and if so, compare them to nonspecific IgG-IRDye800CW. Tail vein injections were administered with one of the three fluorescently-labeled antibodies or IgG (200 μ g). For the human STSGs, samples were obtained by informed consent for patients undergoing head and neck cancer surgery. Tissue samples approximately 2 \times 2 cm in size were transported on ice from the operating room to the lab. Skin from the back of a nude mouse was then excised. The skin graft was then sutured into place and monitored for satisfactory uptake. Once graft survival was ensured, each mouse was systemically injected with one of the labeled antibodies. As previously demonstrated, this was done in order to determine the expected background fluorescence in humans.^{13,15,16}

In the ear model, 3 mice were injected on the dorsal side of the ear with A375 cells. Tumor size was monitored and tail vein injections were performed with one of the three labeled antibodies. Mice were then imaged by SPY and Pearl for 21 days to assess peak fluorescence and stability of each labeled antibody over time. Because the Pearl adjusts the range of fluorescence to optimize the image, ranges were standardized (0.00E⁰ to -4.34E⁻¹)

for all mice over 21 days for objective comparison. Fluorescence intensity was quantified using ImageJ software.¹⁷ Several regions of interest (ROI) within the tumor were selected using an equal-sized circle and a mean value was calculated. The same technique was used to measure background (defined as adjacent normal tissue within 1 cm of tumor) fluorescence intensity. TBRs were then calculated.

Finally, the ear model was used for the surgical resections as it allows for both lymphatic and hematogenous spread and has been shown to accurately represent metastatic melanoma.¹⁸ 18 mice received injections of the appropriate cell line on the dorsal ear. Mice were then injected with one of the three labeled antibodies; three mice per antibody in each cell line. TBRs were calculated.

Fluorescent Imaging and Measurement

The sequence of real-time fluorescent-guided resection and positive specimen confirmation by a second fluorescent imager is illustrated in Figure 1. The SPY imaging system captures fluorescent light using a charged couple device video camera at a rate of 30 frames/second, allowing the user to visualize images in real time on a computer monitor.¹⁹ This system was used to guide tumor resections 48 hours post antibody-dye conjugate injections. Mice were also imaged with the Pearl. Additional imaging allowed for co-localization and verification of fluorescence seen by the SPY. Following resections, excised tissues were placed in tissue cassettes and imaged with both modalities.

Microscopic Fluorescent Imaging

Images were obtained by fluorescence microscopy using an Olympus IX81 Inverted Microscope equipped with a halogen bulb and NIR filter cube (EXHQ760/40X, 790 dcxr, EMHQ830/50m; Chroma Technology Corp., Rockingham, VT).

Statistical Analysis

For each cell line, TBRs of each antibody were compared using a one-way ANOVA test with a Tukey's post-test using GraphPad Prism version 5.04 for Windows (GraphPad Software, San Diego, California USA). Statistical analysis was performed by the lead author and significance was considered $p < 0.05$.

Results

Specificity of Bevacizumab, Panitumumab and Tocilizumab for Imaging Melanoma

To determine the corresponding antigen expression for each antibody in our model, protein analysis of melanoma cell line tumors grown *in vivo* and normal skin samples was assessed by western blotting for the proteins of interest (Supplemental Figure 1). EGFR, VEGF, and IL-6R, demonstrated strong expression in the A375 and SKMEL5 cell line tumors grown *in vivo*. We then evaluated whether our fluorophore-labeled antibodies retained antigen specificity *in vitro* using an optical scatchard analysis (data not shown). Each antibody maintained antigen specificity after IRDye800CW labeling. The binding affinity of labeled antibody was assessed at 8 different concentrations and was found to approach that of the unconjugated antibody (Supplemental Figure 2).

NIR Fluorescent Imaging of Tumors

In vivo specificities were evaluated by comparing uptake of fluorescently-labeled antibodies to the uptake of nonspecific IgG-IRDye800CW in mice with A375 flank tumors. Tumor fluorescence was evaluated and compared using both SPY and Pearl. As we have shown in other tumor types,^{13, 15, 16} labeled IgG does not achieve notable contrast and this was again

true in melanoma tumors. This data implies that better tumor specificity exists with fluorescently-labeled antibodies.

To determine expected background fluorescence in humans, the uptake of each antibody-dye conjugate was evaluated in human STSGs. The human STSGs showed comparable background fluorescence to mouse skin (data not shown). This suggested that all three labeled antibodies would exhibit TBRs sufficient to guide surgical resections in humans.

Three mice with A375 tumors were imaged daily for 21 days to assess peak fluorescence of each fluorescently-labeled antibody as well as stability over time. Figure 2 illustrates the fluorescence intensities achieved. Intensity ranges were standardized for fair comparison on the Pearl imager; therefore, tumor fluorescence saturation occurs during the first few days and normalizes over time. Panitumumab achieved the highest TBRs with both SPY and Pearl (3.8 and 6.6) on days 8 and 20, respectively. Next was bevacizumab with TBRs of 3 and 5.8 on SPY and Pearl, while tocilizumab only attained TBRs of 2.9 and 5.1. SPY's fluorescent peaks occurred between days 5 and 9 for the three antibodies, while they occurred much later (between days 15 and 20) using the Pearl. By day 21, panitumumab still had enough contrast to produce TBRs of 2.5 and 6.5 (SPY, Pearl). Bevacizumab and tocilizumab were lower at day 21 (1.9 and 4.9; 1.4 and 3.4). This data suggested that panitumumab would perform best over time.

In the ear model, all fluorescently-labeled antibodies achieved sufficient contrast to guide surgical resection (Figure 3A). Comparing antibodies against each other, however, we found no significant difference with either imaging modality or cell line (A375: $p=0.27$ SPY, $p=0.72$ Pearl; SKMEL5 $p=0.41$ SPY, $p=0.08$ Pearl; one-way ANOVA). On further analysis, a Tukey's post-test also did not reveal any differences among antibodies. Therefore, all three antibodies produced appreciable TBRs in the ear model, signifying clear differentiation from healthy background tissue. Specific values for each antibody in each cell line are as follows:

In the A375 cell line tumors ($n=9$), tocilizumab achieved the highest TBR of 1.6 using the SPY while bevacizumab achieved a TBR of 3.4 with the Pearl. TBR ranges for SPY and Pearl were 1.4-1.6 and 2.4-3.4 respectively. In the SKMEL5 tumors ($n=9$), the findings were similar. Tocilizumab attained the best TBR (1.9) using the SPY and bevacizumab was best with the Pearl (3.0). SPY and Pearl ranges for tumors was 1.6-1.9 and 2.3-3, respectively (Figure 3B).

Resection Using NIR Fluorescence-Guided Imaging

For each mouse, initial tumor imaging using both modalities was performed prior to any resection. Next, the primary tumor was resected in real-time under the guidance of the SPY. SPY imaging for the primary tumor resection was then compared to images obtained with the Pearl imager. The wound bed was then re-imaged by both modalities for residual fluorescent areas and the SPY was again used in the real-time resection of these fluorescently positive areas. As demonstrated in Figure 4A, fluorescently-labeled bevacizumab and panitumumab were able to identify residual disease (0.5×0.4 cm and 0.6×0.6 cm respectively) after primary tumor resections. Under white light, it was unclear if these areas were tumor or not. The SPY and Pearl revealed fluorescence in these areas and residual tissue samples were later confirmed for the presence of melanoma by pathologic examination and HMB-45 staining. With tocilizumab, an axillary lymph node fluoresced and was presumed to be positive for metastasis at the time of resection. As shown in Figure 4B, the primary tumor was removed in 2 pieces and placed in a tissue cassette, while a remaining fluorescent area in the axilla was detected by both modalities. This lymph node, however, proved to be negative for melanoma. After tissue processing, positive tumor slides were imaged with an NIR filter fitted microscope to ascertain dye localization within the

tumor (Figure 5). Images of negative control tissues confirmed specific antibody-dye localization in tumor tissue. Labeled panitumumab appears to collect in the capillary vasculature of the tumor, whereas bevacizumab and tocilizumab show a more diffuse distribution pattern with areas of intense accumulation throughout. The perivascular binding of panitumumab could represent either EGFR on endothelial cells or on tumor cells surrounding the capillaries. Our images show the labeled antibodies specifically binding tumor parenchyma as opposed to the periphery²⁰ and that mechanistically helps understand where the antibody is binding.

Discussion

Identification of microscopic disease in the operating room remains a critical need to improve surgical outcomes. A melanoma-specific optical contrast agent has the potential to fulfill this need by guiding surgical resections in real-time. Here we present data on three fluorophore-labeled antibodies for tumor targeting. Though one did not prove to be significantly better than the other, all achieved higher TBRs and better contrast compared to labeled nonspecific IgG antibody. Furthermore, tumors but not normal human xenografted epithelium showed intense fluorescence. In two cases, bevacizumab and panitumumab were able to identify residual disease and provided improved tumor resections based on pathological evidence. Fluorescence intensities of these two antibodies also proved robust for weeks in serial imaging studies. Conversely, tocilizumab proved to be less specific and its fluorescence intensity was consistently weaker than the others.

Recently, considerable research has emerged on the development of cancer-specific optical contrast agents that could be used in the operating room to guide surgical resections.²¹ Fluorescent imaging of melanoma has concentrated on sentinel lymph node mapping versus primary lesions.²²⁻²⁶ Because of its locally aggressive nature however, primary tumor resections cannot be ignored. Optical imaging holds great promise in improving primary tumor resections and could significantly impact melanoma patient outcomes. Tumor-targeting, however, is a particular challenge in melanoma where no consistent biomarker has yet emerged. In prostate cancer, for example, prostate-specific membrane antigen (PSMA) is abundantly expressed on both the surface and within prostate tumors. This presents itself as an ideal tumor targeting ligand and has shown promise in fluorescent imaging studies.^{27,28} Because no such marker exists for melanoma and given our previous successes with conjugated antibodies,^{10,11,13} we evaluated the use of FDA-approved antibodies in fluorescent-guided resections of primary melanoma tumors. Because of their established pharmacokinetics and safety in humans, antibodies carry a greatly reduced risk for clinical translation. They also confer the advantage of a longer half-life, which allows for better accumulation within tumors over days. In fact, high sensitivity in optical imaging is related to the probe's ability to accumulate and be retained in a targeted area.²⁹ Antibodies therefore, present themselves as a promising tumor-targeting technique.

Imaging in the near infrared spectral range (700-900nm) also imparts particular advantages for melanoma. Not only does this range decrease autofluorescence by decreasing interference from solvents and biomolecules, but it also allows for further penetration into the tissues.²⁹ This is of extreme importance in melanoma, where depth of invasion has prognostic implications. Unfortunately, few approved NIR fluorescent agents specifically designed for conjugation to targeting molecules exist. Cy5.5 and IRDye800CW are two such agents being investigated for clinical applications of optical imaging. IRDye800CW has demonstrated better tissue penetration and produces improved TBRs compared to Cy5.5.³⁰ Furthermore, IRDye800CW has an absorption and emission peak very similar to that of indocyanine green (ICG), a dye commonly used by plastic surgeons for intraoperative angiography. The SPY imaging system used in this study is one such device designed for

that purpose and is available at many tertiary care institutions (either as purchase or lease).³¹ By using this imaging technology, our approach differs from many other groups.^{32,33} The use of pre-existing technology facilitates cost-effective implementation in operating rooms since investment in additional equipment is not required. Co-opting existing antibody targeting technology also differs from other approaches by leveraging current FDA approvals and safety information.

While the labeled antibodies proved successful at delineating tumor from healthy tissue and EGFR, VEGF, and IL-6R were overexpressed in western blot analysis of tumor tissue, it should be noted that they are not melanoma specific. This was particularly noticeable when imaging with tocilizumab. Since IL-6 is a multifunctional cytokine that regulates immune responses and acute phase reactions,³⁴ its receptor may not be a very specific tumor marker. Another limitation may have been the circumscribed nature of the mouse tumors. Though nodular subtypes of melanoma do exist, this tumor quality did not simulate of the often infiltrative nature of melanoma seen in humans. Finally, our chosen fluorophore of IRDye800CW is not currently approved for human use and poses a barrier to clinical translation. The only approved NIR fluorophore in the U.S. for humans (ICG) is unfortunately unable to label targeting agents. However, a promising study by Marshall et al has demonstrated no toxic or adverse effects of IRDye800CW in rats in doses up to 20 mg/kg.³⁵

Conclusion

In conclusion, our data show antibodies to be an effective tumor targeting strategy in NIR real-time fluorescent imaging of melanoma. Benefits of this strategy include the utilization of FDA approved agents with better accumulation in tumors and use of current intraoperative hardware. This research merits continued investigations.

Supplementary Material

Refer to Web version on PubMed Central for supplementary material.

Acknowledgments

Work was supported by grant from NIDCR (R21DE019232) and NIH (T32CA091078-11). Equipment was donated by Novadaq and IRDye800CW was supplied by LI-COR Biosciences. The authors wish to thank Yolanda Hartman for running the Western blot assays and Dr. Andra Frost in the Department of Pathology for assisting in histologic analysis.

References

1. Tannous Z, Al-Arashi M, Shah S, Yaroslavsky AN. Delineating melanoma using multimodal polarized light imaging. *Lasers Surg Med.* Jan; 2009 41(1):10–16. [PubMed: 19143015]
2. Urist MM, Balch CM, Soong SJ, et al. Head and neck melanoma in 534 clinical Stage I patients. A prognostic factors analysis and results of surgical treatment. *Ann Surg.* Dec; 1984 200(6):769–775. [PubMed: 6508408]
3. O'Brien CJ, Coates AS, Petersen-Schaefer K, et al. Experience with 998 cutaneous melanomas of the head and neck over 30 years. *Am J Surg.* Oct; 1991 162(4):310–314. [PubMed: 1951880]
4. Chang KH, Dufresne R Jr, Cruz A, Rogers GS. The operative management of melanoma: where does Mohs surgery fit in? *Dermatol Surg.* Aug; 2011 37(8):1069–1079. [PubMed: 21585592]
5. Trotter MJ. Melanoma margin assessment. *Clin Lab Med.* Jun; 2011 31(2):289–300. [PubMed: 21549242]
6. El Tal AK, Abrou AE, Stiff MA, Mehregan DA. Immunostaining in Mohs micrographic surgery: a review. *Dermatol Surg.* Mar; 2010 36(3):275–290. [PubMed: 20100275]

7. Keereweer S, Kerrebijn JD, Mol IM, et al. Optical imaging of oral squamous cell carcinoma and cervical lymph node metastasis. *Head Neck*. Oct 10.2011
8. Mimeault M, Batra SK. Novel biomarkers and therapeutic targets for optimizing the therapeutic management of melanomas. *World J Clin Oncol*. Mar 10; 2012 3(3):32–42. [PubMed: 22442756]
9. Gu F, Qureshi AA, Niu T, et al. Interleukin and interleukin receptor gene polymorphisms and susceptibility to melanoma. *Melanoma Res*. Oct; 2008 18(5):330–335. [PubMed: 18781131]
10. Gleysteen JP, Duncan RD, Magnuson JS, Skipper JB, Zinn K, Rosenthal EL. Fluorescently labeled cetuximab to evaluate head and neck cancer response to treatment. *Cancer Biol Ther*. Aug; 2007 6(8):1181–1185. [PubMed: 17637562]
11. Withrow KP, Newman JR, Skipper JB, et al. Assessment of bevacizumab conjugated to Cy5.5 for detection of head and neck cancer xenografts. *Technol Cancer Res Treat*. Feb; 2008 7(1):61–66. [PubMed: 18198926]
12. Lee SB, Hassan M, Fisher R, et al. Affibody molecules for in vivo characterization of HER2-positive tumors by near-infrared imaging. *Clin Cancer Res*. Jun 15; 2008 14(12):3840–3849. [PubMed: 18559604]
13. Heath CH, Deep NL, Sweeny L, Zinn KR, Rosenthal EL. Use of Panitumumab-IRDye800 to Image Microscopic Head and Neck Cancer in an Orthotopic Surgical Model. *Ann Surg Oncol*. Nov; 2012 19(12):3879–3887. [PubMed: 22669455]
14. Biosciences, LC. 2007IRDye(R) 800 CW protein labeling kit-- high MW. Lincoln, NE: Li-Cor Biosciences; 2007. p. 1-9.
15. Kulbersh BD, Duncan RD, Magnuson JS, Skipper JB, Zinn K, Rosenthal EL. Sensitivity and specificity of fluorescent immunoguided neoplasm detection in head and neck cancer xenografts. *Arch Otolaryngol Head Neck Surg*. May; 2007 133(5):511–515. [PubMed: 17520766]
16. Rosenthal EL, Kulbersh BD, Duncan RD, et al. In vivo detection of head and neck cancer orthotopic xenografts by immunofluorescence. *Laryngoscope*. Sep; 2006 116(9):1636–1641. [PubMed: 16954995]
17. Bobek V, Kolostova K, Pinterova D, et al. A clinically relevant, syngeneic model of spontaneous, highly metastatic B16 mouse melanoma. *Anticancer Res*. Dec; 2010 30(12):4799–4803. [PubMed: 21187455]
18. Schneider CA, Rasband WS, Eliceiri KW. NIH Image to ImageJ: 25 years of image analysis. *Nat Methods*. Jul; 2012 9(7):671–675. [PubMed: 22930834]
19. Reuthebuch O, Haussler A, Genoni M, et al. Novadaq SPY: intraoperative quality assessment in off-pump coronary artery bypass grafting. *Chest*. Feb; 2004 125(2):418–424. [PubMed: 14769718]
20. Mieog JS, Hutteman M, van der Vorst JR, et al. Image-guided tumor resection using real-time near-infrared fluorescence in a syngeneic rat model of primary breast cancer. *Breast Cancer Res Treat*. Aug; 2011 128(3):679–689. [PubMed: 20821347]
21. Keereweer S, Kerrebijn JD, van Driel PB, et al. Optical image-guided surgery--where do we stand? *Mol Imaging Biol*. Apr; 2011 13(2):199–207. [PubMed: 20617389]
22. Uhara H, Yamazaki N, Takata M, et al. Applicability of radiocolloids, blue dyes and fluorescent indocyanine green to sentinel node biopsy in melanoma. *J Dermatol*. Apr; 2012 39(4):336–338. [PubMed: 21933261]
23. Fujisawa Y, Nakamura Y, Kawachi Y, Otsuka F. Indocyanine green fluorescence-navigated sentinel node biopsy showed higher sensitivity than the radioisotope or blue dye method, which may help to reduce false-negative cases in skin cancer. *J Surg Oncol*. Jul 1; 2012 106(1):41–45. [PubMed: 22252373]
24. Brouwer OR, Klop WM, Buckle T, et al. Feasibility of sentinel node biopsy in head and neck melanoma using a hybrid radioactive and fluorescent tracer. *Ann Surg Oncol*. Jun; 2012 19(6):1988–1994. [PubMed: 22207047]
25. Bradbury MS, Phillips E, Montero PH, et al. Clinically-translated silica nanoparticles as dual-modality cancer-targeted probes for image-guided surgery and interventions. *Integr Biol (Camb)*. Nov 9.2012
26. van der Vorst JR, Schaafsma BE, Verbeek FP, et al. Dose Optimization for Near-Infrared Fluorescence Sentinel Lymph Node Mapping in Melanoma Patients. *Br J Dermatol*. Oct 18.2012

27. Chen Y, Pullambhatla M, Banerjee SR, et al. Synthesis and Biological Evaluation of Low Molecular Weight Fluorescent Imaging Agents for the Prostate-Specific Membrane Antigen. *Bioconjug Chem.* Dec 4.2012
28. Nakajima T, Mitsunaga M, Bander NH, Heston WD, Choyke PL, Kobayashi H. Targeted, activatable, in vivo fluorescence imaging of prostate-specific membrane antigen (PSMA) positive tumors using the quenched humanized J591 antibody-indocyanine green (ICG) conjugate. *Bioconjug Chem.* Aug 17; 2011 22(8):1700–1705. [PubMed: 21740058]
29. Hadjipanayis CG, Jiang H, Roberts DW, Yang L. Current and future clinical applications for optical imaging of cancer: from intraoperative surgical guidance to cancer screening. *Semin Oncol.* Feb; 2011 38(1):109–118. [PubMed: 21362519]
30. Adams KE, Ke S, Kwon S, et al. Comparison of visible and near-infrared wavelength-excitable fluorescent dyes for molecular imaging of cancer. *J Biomed Opt.* Mar-Apr;2007 12(2):024017. [PubMed: 17477732]
31. Gurtner GC, Jones GE, Neligan PC, et al. Intraoperative laser angiography using the SPY system: review of the literature and recommendations for use. *Ann Surg Innov Res.* Jan 7.2013 7(1):1. [PubMed: 23289664]
32. Keereweer S, Kerrebijn JD, Mol IM, et al. Optical imaging of oral squamous cell carcinoma and cervical lymph node metastasis. *Head Neck.* Jul; 2012 34(7):1002–1008. [PubMed: 21987435]
33. van der Vorst JR, Schaafsma BE, Verbeek FP, et al. Near-infrared fluorescence sentinel lymph node mapping of the oral cavity in head and neck cancer patients. *Oral Oncol.* Jan; 2013 49(1):15–19. [PubMed: 22939692]
34. Kishimoto T. The biology of interleukin-6. *Blood.* Jul; 1989 74(1):1–10. [PubMed: 2473791]
35. Marshall MV, Draney D, Sevick-Muraca EM, Olive DM. Single-dose intravenous toxicity study of IRDye 800CW in Sprague-Dawley rats. *Mol Imaging Biol.* Dec; 2010 12(6):583–594. [PubMed: 20376568]

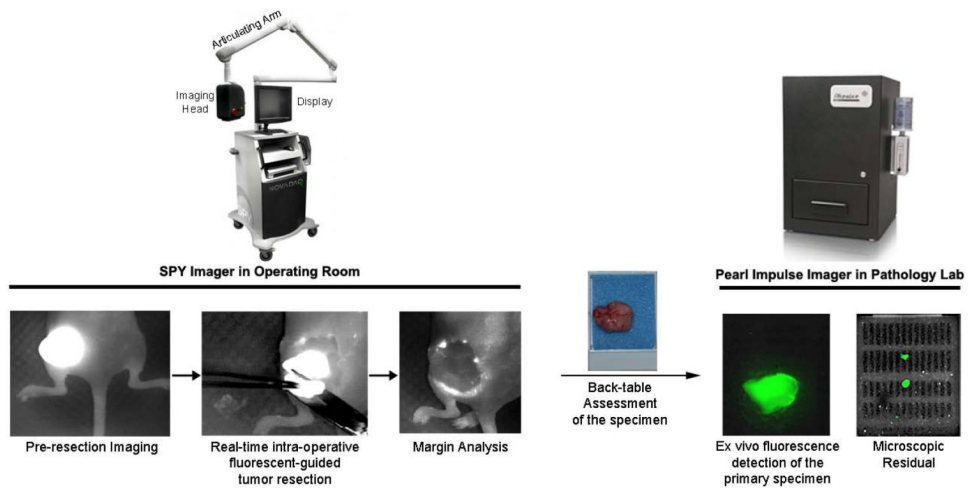


Figure 1. Proposed clinical work flow of fluorescent guided surgery

Fluorescence is observed by SPY optical device in vivo prior to and during surgical resection. Tissue sent to pathology could then be assessed in the small animal Pearl Impulse imager.

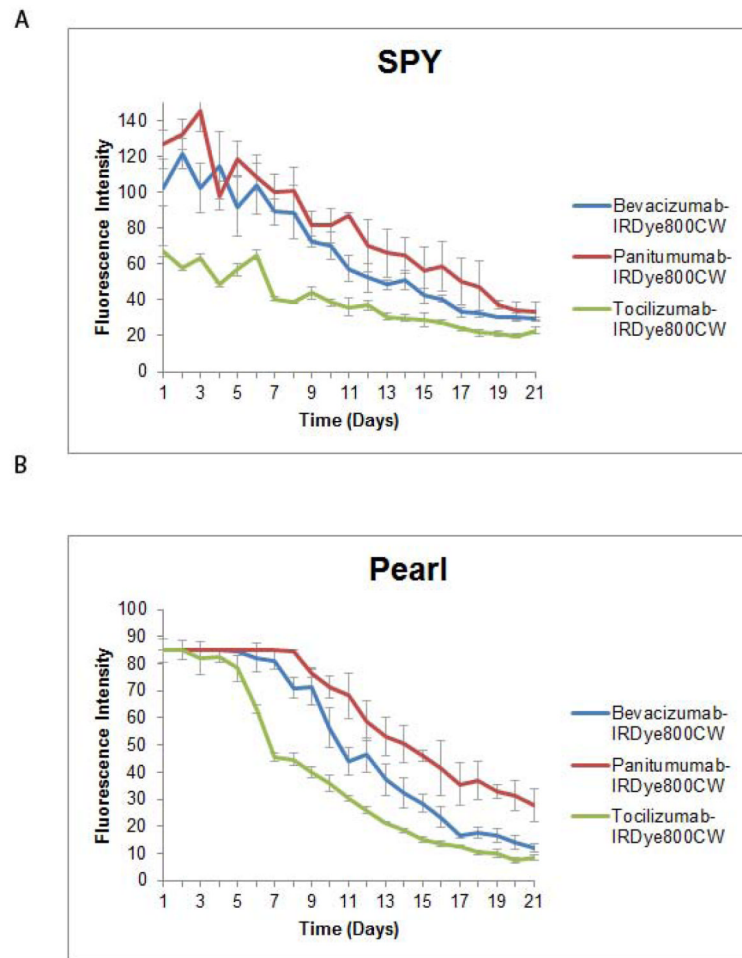


Figure 2. Daily imaging of ear tumors

Orthotopic periauricular A375 tumors were generated and fluorescence intensities were then evaluated for each antibody with SPY (A) and Pearl (B) for 21 days. All intensities decreased over time, but were strong for approximately a week or more.

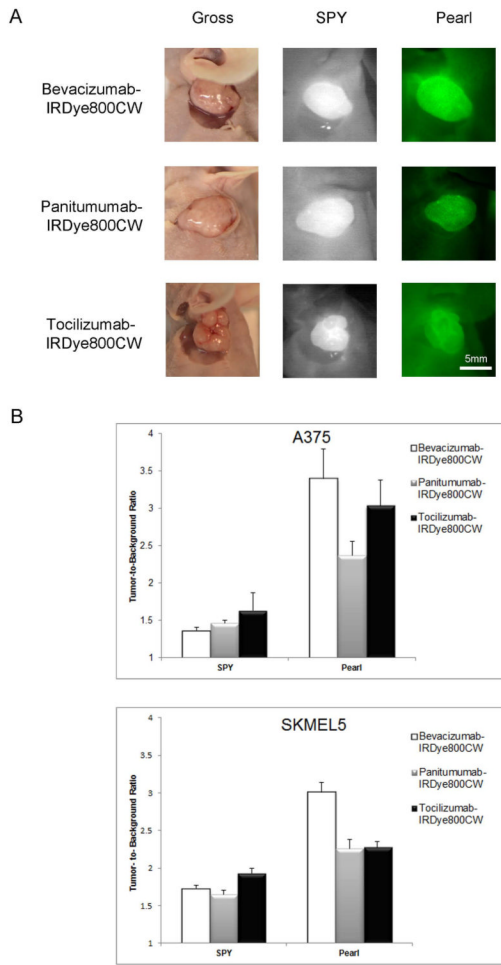


Figure 3. Ear model tumors and TBRs

Representative tumors (SKMEL5) and images are shown for each antibody in the ear model (A). There was no significant difference with the SPY imaging system. Bevacizumab performed best with the Pearl, but this result was also not significant (B).

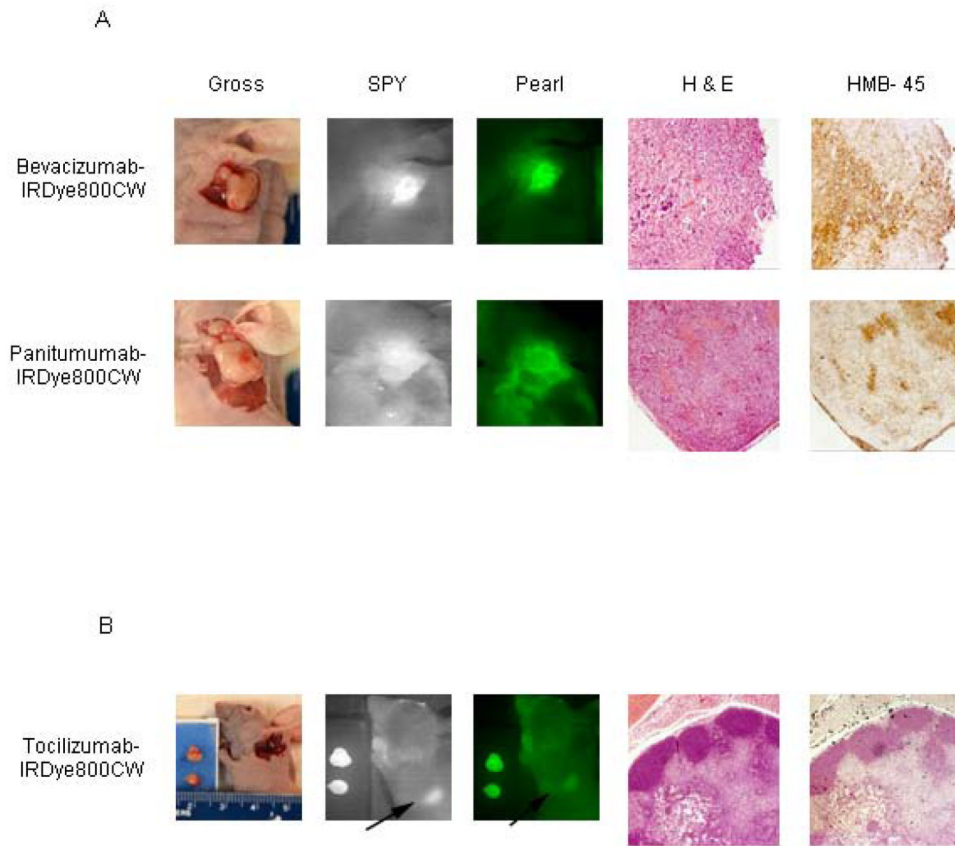


Figure 4. Residual disease detection

Labeled bevacizumab and panitumumab detected residual melanoma that was later confirmed by pathologic assessment and HMB-45 immunostaining (A). Tocilizumab, however, identified an axillary lymph node (denoted by arrows) by imaging, but was later found to be negative for tumor (B).

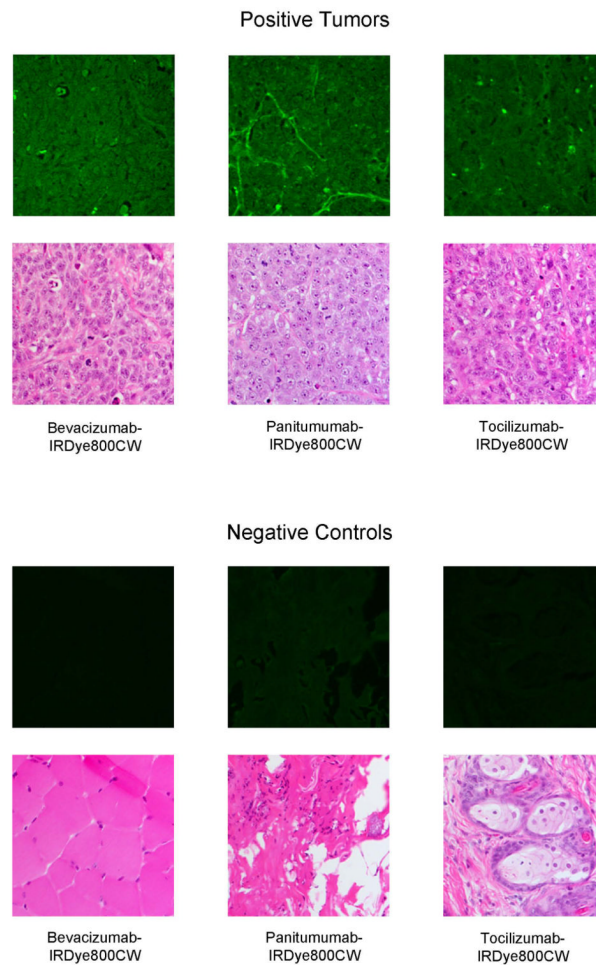


Figure 5. Fluorescent microscopy of ear tumor tissue

A375 tumors were harvested 3 days after systemic injection of antibody-dye conjugate and then processed for histology. Fluorescent microscopy with emission and absorption specific for IRDye800CW was used to localize the pattern of antibody uptake within the tumor.

Table 1
Antibody profiles

FDA- approved antibody	Protein target	Type of antibody	Approved for use in:
Avastin (bevacizumab)	VEGF	Recombinant humanized	mCRC, mRCC, NSCLC, glioblastoma
Vectibix (panitumumab)	EGFR	Fully human	mCRC
Actemra (tocilizumab)	IL-6R	Recombinant humanized	Rheumatoid arthritis

mCRC=metastatic colorectal cancer; mRCC= metastatic renal cell carcinoma; NSCLC= non- small cell lung cancer

Outline of experimental models**Table 2**

Flank model	Experimental mode Comparison of tumors to STSG Comparison of antibodies to IgG
Orthotopic ear model	Surgical model Comparison of antibodies Surgical resections Serial imaging